Photochemical and Chemical Electron Transfer Reactions of Bicyclo[2.1.0]pentanes (Housanes) in Solution and in Zeolite Cavities

Waldemar Adam,[†] Avelino Corma,[‡] Miguel A. Miranda,[‡] María-José Sabater-Picot,[†] and Coskun Sahin*,[†]

Contribution from the Institut für Organische Chemie, Universität Würzburg, Am Hubland, D-97074 Würzburg, Germany, and Instituto de Tecnología Química UPV-CSIC, Universidad Politécnica de Valencia, Camino de Vera S/n, 46071 Valencia, Spain

Received February 6, 1995[⊗]

Abstract: Photochemical electron transfer (PET) and chemical electron transfer (CET) studies have been conducted in solution and within zeolite cavities for the bicyclo[2.1.0]pentanes (**2a**−**j**), prepared by direct photolysis of the corresponding azoalkanes **1**. The advantage of the CET oxidations is that they proceed catalytically in a clean manner to afford the rearranged cyclopentenes **3** in excellent yields. A complete reversal in the regioselectivity of the 1,2 migration has been observed for the unsymmetrical derivatives of bicyclo[2.1.0]pentane, namely **2b** (methyl substitution) *versus* **2c**,**i** (phenyl substitution). Both in solution and in the zeolite cavities, the less substituted cyclopentene **3b′** is obtained for the methyl derivative **2b** and the more substituted cyclopentenes **3c**,**i** for the phenyl cases **2c**,**i**. This unexpected fact is rationalized in terms of delocalization of the positive charge into the aromatic ring for the phenyl-substituted radical cation, as corroborated by AM1 calculations. Furthermore, the electron transfer results of stereolabeled housanes demonstrate that for the deuterium-labeled bridgehead dialkyl-substituted housane **2e**(D) also the *stereochemical memory effect* operates. In contrast, for the methyl-labeled housanes *anti*- and *syn*-**2h**, exclusively hydrogen migration occurs. This differing behavior is interpreted in terms of facile ring inversion of the *syn*-**2h**$^{\bullet+}$ radical cation to the more stable *anti* isomer and subsequent preferential migration of the pseudo-axial hydrogen atom. Moreover, the heterogeneous PET chemistry of the bicyclopentanes **2** in the zeolites establishes convincingly that tailor-made, encapsulated electron transfer photosensitizers serve as effective electron acceptors on optical excitation. In spite of the inherent diffusion problems in such solid sensitizers, quite efficient PET activity is observed compared to that in the homogeneous phase. Unfortunately, the steric confinement imposed by the zeolite support is not sufficient for the small bicyclopentanes, which penetrate into the zeolite interior, to promote selective rearrangements of the radical cation intermediates.

Introduction

Photoinduced electron transfer (PET) is of current interest, and numerous electron transfer sensitizers have been employed not only for mechanistic but also for synthetic purposes.[1,2] The dynamics of these PET processes imply the intermediacy of donor−acceptor (A = acceptor, D = donor) entities characterized by the intermolecular distance and the degree of charge separation (eq 1). The formation of molecular species such as

$$A^* + D \rightleftharpoons [A^{\bullet-}/D^{\bullet+}] \rightleftharpoons A^{\bullet-} + D^{\bullet+} \qquad (1)$$

contact ion pairs (CIP), solvent-separated ion pairs (SSIP), and free ions (FI) have been documented.[1,2] It is known that the reactivities of these intermediates differ since some chemical events occur exclusively at the CIP, SSIP, or FI stage. The mechanistic complexities in the chemical fate of the resulting radical ion species are illustrated in the alternative reaction channels for the PET reaction of bicyclo[2.1.0]pentanes (Scheme 1).[3] As a matter of fact, the yield of photoproduct depends to a high degree on the lifetime of the radical ions, which is fixed by the rate of electron back-transfer (BET). Therefore, product formation is only feasible if one can effectively decrease the rate of BET.[2e,4] An effective method for photoinduced electron transfer to generate more persistent radical ions, is the co-sensitization technique (eq 2).[2c,5] The advantage by employing

[†] University of Würzburg.
[‡] University of Valencia.
[⊗] Abstract published in *Advance ACS Abstracts,* March 1, 1996.

(1) (a) Kavarnos, G. J.; Turro, N. J. *Chem. Rev.* **1986**, *86*, 401−449. (b) Sakuragi, H.; Nakagaki, R.; Oguchi, T.; Arai, T.; Tokumaru, K.; Nagakura, S. *Chem. Phys. Lett.* **1987**, *135*, 325−329. (c) Oguchi, T.; Arai, T.; Sakuragi, H.; Tokumaru, K. *Bull. Chem. Soc. Jpn.* **1987**, *60*, 2395−2399. (d) Julliard, M.; Chanon, M. *Chem. Rev.* **1983**, *83*, 425−506. (e) Fox, M. A., Chanon, M., Eds. *Photoinduced Electron Transfer*; Elsevier: Amsterdam, 1988.

(2) (a) Mattay, J. *Angew. Chem., Int. Ed. Engl.* **1987**, *26*, 825−845. (b) Mattay, J. *Synthesis* **1989**, 223−252. (c) Farid, S.; Mattes, S. L. In *Organic Photochemistry*; Padwa, A., Ed.; Marcel Dekker: New York, 1983; Vol. 6, pp 233−326. (d) Fox, M. A. In *Advanced Photochemistry*; Volman, D. H., Hammond, G. S., Gollnick, K., Eds.; J. Wiley & Sons: New York, 1986; Vol. 13, pp 237−327. (e) Kavarnos, G. J. *Top. Curr. Chem.* **1990**, *156*, 21−58.

(3) (a) Adam, W.; Sahin, C.; Sendelbach, J.; Walter, H.; Chen, G.-F.; Williams, F. *J. Am. Chem. Soc.* **1994**, *116*, 2576−2584. (b) Adam, W.; Sendelbach, J. *J. Org. Chem.* **1993**, *58*, 5316−5322. (c) Adam, W.; Sendelbach, J. *J. Org. Chem.* **1993**, *58*, 5310−5315. (d) Adam, W.; Denninger, U.; Finzel, R.; Kita, F.; Platsch, H.; Walter, H.; Zang, G. *J. Am. Chem. Soc.* **1992**, *114*, 5027−5035. (e) Adam, W.; Walter, H.; Chen, G.-F.; Williams, F. *J. Am. Chem. Soc.* **1992**, *114*, 3007−3014. (f) Adam, W.; Dörr, M. *J. Am. Chem. Soc.* **1987**, *109*, 1570−1572.

(4) Gould, I. R.; Young, R. H.; Moody, R. E.; Farid, S. *J. Phys. Chem.* **1991**, *95*, 2068−2080.

(5) (a) Gould, I. R.; Ege, D.; Mooser, J. E.; Farid, S. *J. Am. Chem. Soc.* **1990**, *112*, 4290−4301. (b) Julliard, M. In *Photoinduced Electron Transfer*; Fox, M. A., Chanon, M., Eds.; Elsevier: Amsterdam, 1988; Part B, pp 216−313. (c) Schaap, A. P.; Siddiqui, S.; Prasad, G.; Palomino, E.; Lopez, L. *J. Photochem.* **1984**, *25*, 167−181. (d) Arnold, D. R.; Snow, M. S. *Can. J. Chem.* **1988**, *66*, 3012−3026. (e) Majiama, T.; Pac, C.; Nakasone, A.; Sakurai, H. *J. Am. Chem. Soc.* **1981**, *103*, 4499−4508.

0002-7863/96/1518-2380$12.00/0

Scheme 1

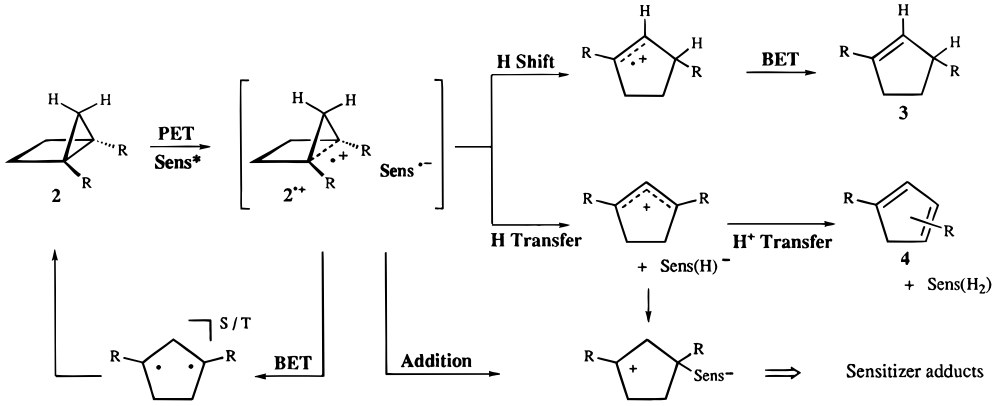

a codonor—in most cases biphenyl—is the spatial separation of the reduced electron acceptor from the desired donor radical cation.

$$A^* + Ph_2 \rightleftharpoons [A^{\bullet-}/Ph_2^{\bullet+}] \rightleftharpoons A^{\bullet-} + Ph_2^{\bullet+} \qquad (2)$$

$$Ph_2^{\bullet+} + D \rightleftharpoons [Ph_2/D^{\bullet+}] \rightleftharpoons Ph_2 + D^{\bullet+}$$

We have previously shown that chemical electron transfer (CET) with tris(aryl)aminium salts constitutes a useful method to minimize BET to 1,3-cyclopentanediyl radical cations derived from bicyclo[2.1.0]pentanes.[6] These tris(aryl)aminium salts are convenient one-electron oxidants, whose oxidation potential can be conveniently tuned by the number of bromine substituents contained in the three aryl rings.[7] The catalytically generated 1,3-diyl radical cations rearrange regioselectively to the corresponding cyclopentenes. Since intermediary D−A radical ion pairs are not formed in the CET compared to the PET mode (eq 3), alternative reaction channels for the 1,3-radical cation are minimized and excellent yields of defined rearrangement products are obtained.[6] Therefore, this oxidative rearrangement methodology may constitute a useful synthetic tool for tailor-made substrates.

$$SbCl_6^- Ar_3N^{\bullet+} + D \rightleftharpoons [SbCl_6^-/Ar_3N/D^{\bullet+}] \rightleftharpoons SbCl_6^- + Ar_3N + D^{\bullet+} \qquad (3)$$

Recently, the 2,4,6-triphenylpyrylium cation (Y[TP$^+$]),[8] a well-established electron acceptor in its excited state,[9] has been entrapped in Y zeolite for heterogeneous PET studies. It was discovered, that the zeolite framework stabilizes the resulting ion pairs and regulates decisively the rate of BET.[10] Thus, such novel heterogeneous sensitizers offer the opportunity to explore the chemical behavior of radical cations in confined spaces.

In the present study, various bicyclo[2.1.0]pentanes **2** were chosen as substrates for the electron transfer reactions in solution and within zeolite cavities. The comparison of the CET and

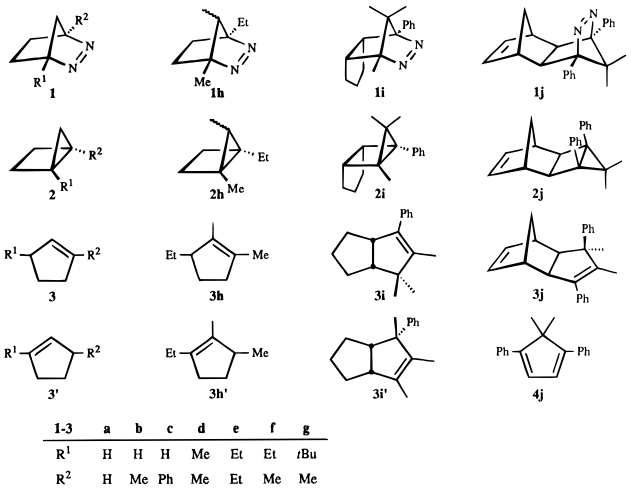

1-3	a	b	c	d	e	f	g
R^1	H	H	H	Me	Et	Et	*t*Bu
R^2	H	Me	Ph	Me	Et	Me	Me

PET modes provides valuable mechanistic insight on the rearrangement of the intermediary 1,3-diyl radical cations. The convenience and scope of CET by tris(aryl)aminium salts is demonstrated in its application to the bicyclo[2.1.0]pentanes **2**.

Results

Synthesis of Starting Materials and Structure Assignments. Synthesis of the Azoalkanes. 2,3-Diazabicyclo[2.2.1]-hept-2-ene (**1a**),[11] 1-methyl-2,3-diazabicyclo[2.2.1]hept-2-ene (**1b**),[12] 1-phenyl-2,3-diazabicyclo[2.2.1]hept-2-ene (**1c**),[13] 1,4-dimethylbicyclo[2.2.1]hept-2-ene (**1d**)[12] and (1α,4α,4aα,5*β*,8*β*,8aα)-1,4,4a,5,8,8a-hexahydro-9,9-dimethyl-1,4-diphenyl-1,4:5,8-dimethanophthalazine (**1j**)[14a] were prepared as reported. The synthesis of the 1,4-dialkylated 2,3-diazabicyclo[2.2.1]hept-2-enes **1e**−**g** with stereolabels at the C-7 position has already been published.[15] The procedure requires *syn* carbometalation of the protected 1-alkynones by dialkylcuprates, followed by hydrolysis of the ketal functionality to afford the *γ*,*δ*-unsaturated ketones. Conversion to the tosylhydrazones followed by BF_3-catalyzed

(6) Adam, W.; Sahin, C. *Tetrahedron Lett.* **1994**, *35*, 9027−9030.
(7) Schmidt, W.; Steckhan, E. *Chem. Ber.* **1980**, *113*, 577−585.
(8) (a) Corma, A.; Fornés, V.; García, H.; Miranda, M. A.; Primo, J.; Sabater, M. J. *J. Am. Chem. Soc.* **1994**, *116*, 2276−2280. (b) Corma, A.; Fornés, V.; García, H.; Miranda, M. A.; Sabater, M. J. *J. Am. Chem. Soc.* **1994**, *116*, 9767−9768. (c) Corma, A.; García, H.; Iborra, S.; Martí, V.; Miranda, M. A.; Primo, J. *J. Am. Chem. Soc.* **1993**, *115*, 2177−2180. (d) Alvaro, M.; Corma, A.; García, H.; Miranda, M. A.; Primo, J. *J. Chem. Soc., Chem. Commun.* **1993**, 1041−1042. (e) Corma, A.; Fornés, V.; Rey, F. *Appl. Catal.* **1990**, *59*, 267−274.
(9) Miranda, M. A.; García, H. *Chem. Rev.* **1994**, *94*, 1063−1089.
(10) (a) Ramamurthy, V., Ed. *Photochemistry in Organized and Constrained Media*; Verlag Chemie: New York, 1991. (b) Ramamurthy, V.; Caspar, J. V.; Corbin, D. R. *J. Am. Chem. Soc.* **1991**, *113*, 594−600. (c) Gessner, F.; Scaiano, J. C. *J. Photochem. Photobiol., A* **1992**, *67*, 91−100. (d) Sankararaman, S.; Yoon, K. B.; Yobe, T.; Kochi, J. K. *J. Am. Chem. Soc.* **1991**, *113*, 1419−1421.
(11) (a) Gassman, P. G.; Mansfield, K. T. *Org. Synth.* **1969**, *49*, 1−6. (b) Criegee, R.; Rimmelin, A. *Chem. Ber.* **1957**, *90*, 414−417.
(12) Wilson, R. M.; Rekers, J. W.; Packard, A. B.; Elder, R. C. *J. Am. Chem. Soc.* **1980**, *102*, 1633−1641.
(13) Adam, W.; Grabowski, S.; Platsch, H.; Hannemann, K.; Wirz, J.; Wilson, R. M. *J. Am. Chem. Soc.* **1989**, *111*, 751−753.
(14) (a) Beck, K.; Hünig, S. *Chem. Ber.* **1987**, *120*, 477−483. (b) Beck, K.; Höhn, A.; Hünig, S.; Prokschy, F. *Chem. Ber.* **1984**, *117*, 517−533.
(15) Adam, W.; Sahin, C.; Schneider, M. *J. Am. Chem. Soc.* **1995**, *117*, 1695−1702.

cyclization to the azoalkanes completes the sequence. The hitherto unknown 1,4-dialkylated azoalkane **1h** with an additional methyl stereolabel at the C-7 position was synthesized by following this protocol. Contrary to the deuterium-labeled cases, the intermediary vinylcuprate had to be first activated with $P(OEt)_3$[16] before the electrophile (CH_3I) was added. For the deuterium-labeled tosylhydrazones, as well as for the methyl-labeled one, the BF_3-catalyzed cyclization process is highly diastereoselective in that the initial *syn*/*anti* diastereomeric ratio of the tosylhydrazone dictates the stereochemical outcome in the final azoalkane. The methyl group at δ 0.43 for the major isomer (83%) of azoalkane **1h** possesses the *syn* configuration (shielding by the proximate azo group[17]), while the corresponding methyl resonance for the minor *anti* isomer is located at δ 0.69. NOE experiments corroborated the proposed stereochemistry. Whereas irradiation of the methyl group of the major isomer at δ 0.43 gave an enhanced intensity only for 7-H_a (2.4%), irradiation of the methyl group of the minor isomer at δ 0.69 increased the 7-H_s (2.5%) and 5,6-H_x (1.5%) resonances.

The tricyclic azoalkane **1i** was synthesized according to the Hünig route.[14] By comparison with the literature spectral data of the two symmetrically substituted derivatives, for the unsaturated precursors, the major regioisomer was assigned the 1-phenyl-4,8,8-trimethyl and the minor the 4-phenyl-1,8,8-trimethyl substitution pattern.

Synthesis of the Bicyclopentanes. The bicyclo[2.1.0]-pentanes **2** were obtained by direct photolysis of the azoalkanes **1** and separated by preparative gas or column chromatography. As for simple DBH-type azoalkanes,[18] the photolysis of azoalkanes **1** afforded exclusively housanes **2** and only traces of olefins **3**. Accordingly, bicyclo[2.1.0]pentane (**2a**),[11b,19] 1-methylbicyclo[2.1.0]pentane (**2b**),[20] 1-phenylbicyclo[2.1.0]pentane (**2c**),[21] 1,4-dimethylbicyclo[2.1.0]pentane (**2d**),[20] and 4,4-dimethyl-3,5-diphenyl-*endo*-tetracyclo[5.2.1.$0^{2,6}$.$0^{3,5}$]dec-8-ene (**2j**)[14] were prepared and their spectral and physical data found to be in accord with those reported. The stereochemical assignment in the deuterium-labeled bicyclo[2.1.0]pentanes **2e**−**g**(D) was confirmed by comparison with the literature spectral data of the parent 1,4-dimethylbicyclo[2.1.0]pentane (**2d**) and on the basis of the characteristic W coupling (J = 1.80−2.04 Hz) only for 5-H_a.[20] Thus, the high-field proton in **2d**−**f** (δ 0.13−0.22) was assigned to 5-H_a and the low-field one (δ 0.61−0.69) to 5-H_s. In contrast, for housane **2g**, the high-field proton (δ 0.39) belongs to 5-H_s and the low-field one (δ 0.56) to 5-H_a. The different chemical shifts presumably derive from the proximity of the bulky *tert*-butyl group. NOE experiments on the bicyclo-[2.1.0]pentanes **2d,g** corroborated the proposed stereochemistry. For housane **2h**, the methyl groups at δ 0.86 and 1.00 were assigned the *anti* and *syn* configurations as confirmed also by NOE experiments.

Electron Transfer Reactions of Bicyclopentanes 2. The product data are summarized in Table 1. Oxidation of the parent bicyclo[2.1.0]pentane **2a** under PET conditions gave a very low mass balance (1%) of cyclopentene **3a** as the only detectable product by GC (entry 1, Table 1); the remainder was undefined higher-molecular-weight material. The highest mass balance was achieved in the photosensitized reaction with encapsulated Y[TP] (entry 2). While complete conversion (entry 3) was observed when housane **2a** was treated with catalytic amounts (2−10 mol %) of the strong oxidant (E_{ox} = 1.50 V *vs* SCE)[7] *tris*(2,4-dibromophenyl)aminium hexachloroantimonate ($TDA^{\bullet+}$), the less powerful (E_{ox} = 1.06 V *vs* SCE)[7] tris(4-bromophenyl)-aminium hexachloroantimonate ($TBA^{\bullet+}$) failed to oxidize this substrate (not shown in Table 1).

Contrary to the parent housane **2a**, the unsymmetrically bridgehead-substituted housanes **2b**,**c** were consumed completely by catalytic amounts of $TBA^{\bullet+}$ (entries 6 and 10). Housane **2b** yielded in all cases the less substituted cyclopentene **3b′** [22] as the major (entry 5) or as the exclusive (entries 4 and 6) oxidation product. The related phenyl-substituted housane **2c** afforded always (entries 7−10) the cyclopentenes **3c**[21] and

Table 1. Product Studies of the Chemical and Photochemical Electron Transfer Reactions for the Bicyclopentanes **2** in Solution and within Zeolite Cavities

							prod dist (%)[b,c]	
entry	substrate	mode[a]	*t* (min)	solvent	conv[b] (%)	mb[b] (%)	**3**	**3′**
1	**2a**	TPT	30	CH_2Cl_2	11	1	100	
2	**2a**	Y[TP]	60	CH_2Cl_2	12	90	100	
3	**2a**	$TDA^{\bullet+}$	1	CH_2Cl_2	100	75	100	
4	**2b**	TPT	5	CH_2Cl_2	23	26		100
5	**2b**	Y[TP]	15	CH_2Cl_2	7	41	33	67
6	**2b**	$TBA^{\bullet+}$	1	CH_2Cl_2	100	89		100
7	**2c**	DCA/Ph_2	10	CH_3CN	31	60	77	23
8	**2c**	TPT	20	CH_2Cl_2	36	57	78	22
9	**2c**	Y[TP]	30	CH_2Cl_2	18	40	80	20
10	**2c**	$TBA^{\bullet+}$	1	$CDCl_3$	100	90	78	22
11	**2d**	DCA/Ph_2	10	CH_3CN	15	60	95	*d*
12	**2d**	$TBA^{\bullet+}$	1	$CDCl_3$	100	95	100	
13	**2e**	TPT	5	CH_2Cl_2	17	58	100	
14	**2e**	Y[TP]	30	CH_2Cl_2	4	50	100	15
15	**2e(D)**[e]	$TBA^{\bullet+}$	1	C_6D_6	100	92	100[e]	
16	**2e(D)**[f]	$TBA^{\bullet+}$	1	C_6D_6	100	95	100[f]	
17	**2f**	TPT	10	CH_2Cl_2	18	51	61	39
18	**2f**	Y[TP]	30	CH_2Cl_2	17	43	57	43
19	**2f**	$TBA^{\bullet+}$	1	CH_2Cl_2	100	91	61	39
20	**2g**	$TBA^{\bullet+}$	1	CH_3CN	100	85	60	40
21	**2h**[g]	TPT	5	CH_2Cl_2	17	73	61	39
22	**2h**[g]	Y[TP]	30	CH_2Cl_2	7	62	50	50
23	**2h**[g]	$TBA^{\bullet+}$	1	CH_2Cl_2	100	89	62	38
24	*anti*-**2h**	$TBA^{\bullet+}$	1	CH_2Cl_2	100	99	62	38
25	*syn*-**2h**	$TBA^{\bullet+}$	1	CH_2Cl_2	100	85	68	32
26	**2i**	TPT	10	$CDCl_3$	20	70	100	
27	**2i**	Y[TP]	30	$CDCl_3$	12	60	100	
28	**2i**	$TBA^{\bullet+}$	1	$CDCl_3$	100	97	100	
29	**2j**	DCA/Ph_2	3	CH_3CN	70	85	27	*h*
30	**2j**	Y[TP]	60	$CDCl_3$	0	0		
31	**2j**	$TBA^{\bullet+}$	1	$CDCl_3$	100	97	27	*h*

[a] TPT = 2,4,6-triphenylpyrylium tetrafluoroborate, Y[TP] = 2,4,6-triphenylpyrylium cation entrapped in the Y zeolite, $TDA^{\bullet+}$ = tris(2,4-bromophenyl)aminium hexachloroantimonate, and $TBA^{\bullet+}$ = tris(4-bromophenyl)aminium hexachloroantimonate. [b] Conversion, mass balance (mb), and product distribution were determined by quantitative capillary GC analysis (error ca. 5% of stated value) or by ^{1}H-NMR spectroscopy (error ca. 10% of stated values). [c] Relative yields normalized to 100%, error ca. 2−5% of the stated values. [d] The remainder 5% is dimethylcyclopentadiene. [e] *syn*/*anti*-**2e**(D) = 42:58 gives a ratio of **3e**(2-D): 3e(3-D) = 58:42 as determined by ^{1}H-NMR spectrosccopy, error ca. 3% of stated value. [f] *syn*/*anti*-**2e**(D) = 48:52 gives a ratio of **3e**(2-D): **3e**(3-D) = 52:48 as determined by ^{1}H-NMR spectroscopy, error ca. 3% of stated value. [g] *syn*/*anti* isomers, ratio = 60:40. [h] 73% 5,5-dimethyl-1,4-diphenylcyclopentadiene (**4j**) and 73% cyclopentadiene were formed.

(16) Usually the cancerogenic hexamethylphosphoric triamide is used in activating vinylcuprates, cf.: Alexakis, A.; Normant, J. *J. Organomet. Chem.* **1975**, *96*, 471−485. Alexakis, A.; Cahiez, G.; Normant, J. F. *Synthesis* **1979**, 826−830.

(17) For related systems see ref. 3e and also the following Paquette, L. A.; Leichter, L. M. *J. Am. Chem. Soc.* **1971**, *93*, 5128−5136.

(18) (a) Adam, W.; DeLucchi, O. *Angew. Chem.* **1980**, *92*, 815−832; *Angew. Chem., Int. Ed. Engl.* **1980**, 762. (b) Engel, P. S. *Chem. Rev.* **1980**, *80*, 99−150.

(19) Adam, W.; Oppenländer, T.; Zang, G. *J. Org. Chem.* **1985**, *50*, 3303−3312.

(20) Wiberg, K. B.; Kass, S. R.; Bishop, K. C., III *J. Am. Chem. Soc.* **1985**, *107*, 996-1002.

(21) McKinney, M. A.; Chou, S. K. *Tetrahedron Lett.* **1974**, 1145−1148.

(22) (a) Descoins, C.; Julia, M.; Sang, H. V. *Bull. Soc. Chim. Fr.* **1971**, 4087−4093. (b) Ohbe, Y.; Matsuda, T. *Bull. Chem. Soc. Jpn.* **1975**, *48*, 2389−2390.

3c′ [23] as rearrangement products, with the higher substituted **3c** as the major regioisomer. The tricyclic housane **2i** gave for all three electron transfer modes (entries 26−28) cyclopentene **3i** as the only rearrangement product.

Control experiments on the cyclopentenes **3b**,**b′** [3e] and **3c**,**c′** confirmed that these olefins did not interconvert into each other under the employed electron transfer conditions. Furthermore, by monitoring the product distribution of the photolyses as a function of time, it has been determined that no secondary oxidation of the cyclopentenes **3** took place up to the conversions stated in Table 1.

For the symmetrical 1,4-dialkylated housanes **2d**,**e**, the CET mode ($TBA^{\bullet+}$) proved to be again more suitable than the photochemical ones in regard to conversion and mass balance (compare entries 12, 15, and 16 *versus* 11, 13, and 14). Thus, complete conversion of the substrates to cyclopentenes **3d** [24] (entry 12) and **3e** [25] (entries 15 and 16) was achieved with catalytic amounts of $TBA^{\bullet+}$. Monitoring of the reaction progress by ^1H NMR spectroscopy revealed that the initial deuterium distribution in the housane **2e**(D) was retained (eq 4) quantitatively (entries 15 and 16) in the cyclopentene product

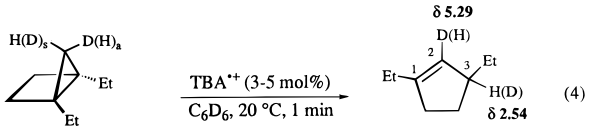

(4)

anti-/*syn*-**2e**(D)	**3e**(3-D) : **3e**(2-D)
58 : 42	**42 : 58**
52 : 48	**48 : 52**

3e(D). The well-separated 5-$H_{a,S}$ resonances for housane **2e**(D) and the 2,3-H resonances for **3e**(D) provided reproducible results in the NMR analysis.

For the unsymmetrical 1,4-dialkylated housanes **2f**−**h**, the expected regioisomeric cyclopentenes **3f**−**h** [25,26] and **3f**−**h′** [27] were obtained in all cases (entries 17−25), with **3f**−**h** as the major regioisomers. Unexpectedly, oxidation of the trialkylated housane **2h** yielded only the two cyclopentenes **3h**,**h′** (entries 21−23) from H shifts, instead of the four possible ones derived from H as well as methyl shifts.

The superiority of the chemical electron transfer mode (complete conversion and higher mass balance) over the photochemical ones was confirmed also for housane **2j** (entries 29 and 31). Both PET and CET yielded olefin **3j** [3c] and the cycloreversion products **4j** [3c,28] and cyclopentadiene. The lack of rearrangement products for the Y[TP] mode (entry 30) confirmed that this bulky housane **2j** did not enter the interior of the zeolite and that outside the zeolite framework no electron transfer process occurs.

The possible involvement of acid-catalyzed rearrangement of the housanes **2** was suppressed by the addition of the hindered base 2,6-di-*tert*-butylpyridine (not shown in Table 1). The unaltered product distributions confirmed that this hindered pyridine interferes with neither the PET nor CET reaction. Contrary to the PET and CET reactions in solution, acid-catalyzed rearrangement was observed with housane **2b** for the Y[TP] mode even in the presence of the hindered base. Only for this extremely acid-sensitive housane does the zeolite framework [8] seem to be acidic enough to catalyze rearrangement in competition with electron transfer.

Location of the 2,4,6-Triphenylpyrylium Cation (TP^+) in the Y-Type Faujasite. This question was assessed by absorption studies with DBH derivatives of different size on protonated Y zeolite (HY). For the small azoalkanes **1a**,**h**, a high percentage (91−100%) of material was absorbed in contrast to the large and bulky azoalkane **1j**. Thus, the azoalkanes **1a,h** have the proper size to penetrate into the interior of the zeolite, whereas the 1,4-diphenyl-substituted azoalkane **1j** remains outside, possibly absorbed on the external surface. Indeed, when the PET reaction of azoalkane **1j** was performed in the heterogeneous phase, hardly any oxidation was observed. This contrasts sharply with the extensive oxidation observed in solution.[3c] Thus, these results suggest that most TP^+ cations are located internally in the cavities.

Discussion

Chemical Electron Transfer of Bicyclopentanes 2. Table 1 reveals convincingly that the CET mode is advantageous for the oxidative rearrangement of the bicyclopentanes **2**. The same chemistry as that for the PET mode is observed, except that the oxidations proceed catalytically in a clean manner to afford the rearranged cyclopentenes **3** in high yields. The lack of alternative reaction channels (see Scheme 1) for the 1,3-radical cation (and the 1,2-radical cation) presumably accounts for the observed clean reactions and the high yields (75−99%) of the CET mode, while in the PET mode, reaction with the reduced photooxidant occurs (low mass balance, side products, etc.).[3] This underscores the advantage of the chemical electron transfer (CET) over the photosensitized (PET) modes.

However, as shown in the Results, at least one bridgehead alkyl or aryl substituent on the bicyclopentane framework is necessary for oxidation by $TBA^{\bullet+}$. Its oxidation power is not sufficient to convert the parent unsubstituted housane **2a** (E_{ox} = 1.91 V).[29] Although the stronger oxidant $TDA^{\bullet+}$ smoothly oxidizes even housane **2a**, its application as electron transfer oxidant is restricted to substrates for which the rearrangement product, in this case the cyclopentene **3**, has an unsubstituted double bond, e.g. the cyclopentenes **3a**,**b′**,**c′**, which are not oxidized further to an intractable higher-molecular-weight material. Fortunately, tri- and tetrasubstituted olefins persist toward $TBA^{\bullet+}$. For this reason, only $TDA^{\bullet+}$ was used to oxidize bicyclopentane **2a** (entry 3).

In all cases examined, catalytic amounts (2−10 mol %) of $Ar_3N^{\bullet+}$ oxidant were enough to achieve complete conversion of the substrate within a few seconds, although the aminium salts possess lower oxidation potentials than the housanes **2**. The driving force presumably derives from the irreversible rearrangement step which follows the endothermic electron transfer process.[30] Therefore, a catalytic cycle is proposed (Scheme 2) in which electron transfer from housane **2** to the aminium salt $Ar_3N^{\bullet+}$ serves for initiation, followed by subsequent 1,2 Wagner−Meerwein rearrangement of the housane radical cation **2**$^{\bullet+}$. The cycle is completed by BET from the

(23) (a) von Braun, J.; Kühn, M. *Ber. Dtsch. Chem. Ges.* **1927**, *60*, 2551−2557. (b) von Braun, J.; Kamp, E.; Kopp, J. *Ibid.* **1937**, *70*, 1750−1760.

(24) Rei, M. H. *J. Org. Chem.* **1978**, *43*, 2173−2178.

(25) Sisido, K.; Kurozumi, S.; Utimoto, K.; Isida, T. *J. Org. Chem.* **1966**, *31*, 2795−2802.

(26) (a) Vaveck, D.; Jaques, J. *Bull. Soc. Chim. Fr.* **1969**, *10*, 3505−3515. (b) Richer, J. C.; Belanger, P. *Can. J . Chem.* **1966**, *44*, 2057−2066.

(27) Gajewski, J. J.; Squicciarini, M. P. *J. Am. Chem. Soc.* **1989**, *111*, 6717−6728.

(28) (a) Adam, W.; Reinhard, G.; Platsch, H.; Wirz, J. *J. Am. Chem. Soc.* **1990**, *112*, 4570−4571. (b) Paquette, L. A.; Leichter, L. M. *J. Org. Chem.* **1974**, *39*, 461−467.

(29) (a) Gassman, P. G.; Yamaguchi, R. *Tetrahedron* **1982**, *38*, 1113−1122. (b) Gassman, P. G.; Yamaguchi, R.; Koser, G. F. *J. Org. Chem.* **1978**, *43*, 4392-4393.

(30) (a) The (irreversible) oxidation potentials for **2a** and **2i** are 1.91 and 1.42 V and the (reversible) ones for TDA and TBA are 1.50 and 1.06 V. The cyclovoltammetric measurements were performed in Prof. M. Schmittel's research group at the University of Würzburg, and we are grateful to H. Trenkle for technical assistance. (b) The (irreversible) oxidation potentials for **3a** and **3i** are 2.03 and 1.58 V.

Scheme 2

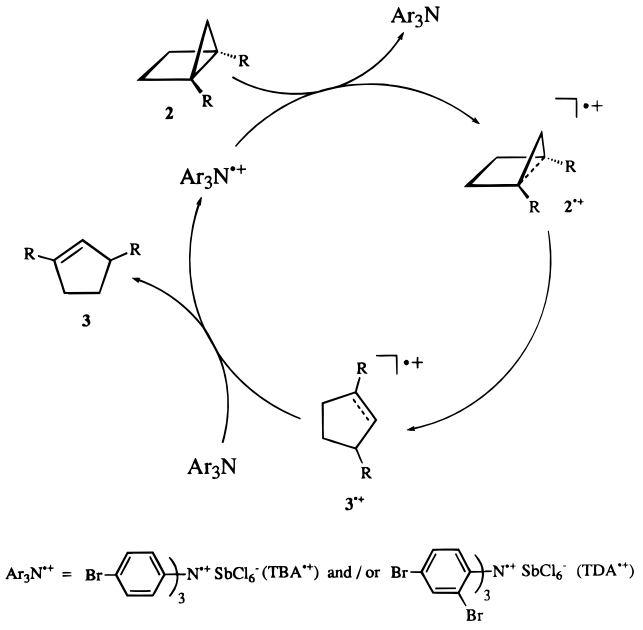

amine Ar_3N to the cyclopentene radical cation **3**$^{\bullet+}$ to form cyclopentene **3** and regenerate the aminium salt $Ar_3N^{\bullet+}$. Alternatively, BET can also occur directly from the housane **2** to **3**$^{\bullet+}$ to yield cyclopentene **3** and a new housane radical cation **2**$^{\bullet+}$ (chain mechanism). However, this mechanistic pathway (ΔE 0.12−0.16 V)[30b] is unlikely in view of the substantial exothermicity for the BET from the amine to the cyclopentene radical cation **3**$^{\bullet+}$ (ΔE ca. 0.5 V) in the catalytic cycle.

Regioselectivity of the 1,2 Migration in the Radical Cations. Analogous to the photochemically and radiolytically induced oxidation of the unsymmetrical methyl-substituted housane **2b**,[3a] the chemical oxidation (entry 6, Table 1) yielded exclusively 3-methylcyclopentene (**3b′**) and no 1-methylcyclopentene (**3b**). This novel contra-thermodynamically regioselective 1,2 hydrogen migration was rationalized in terms of a preferentially localized partial positive charge at the incipient tertiary center of the 1,3-diyl radical cation **2b**$^{\bullet+}$. Contrary to the methyl case **2b** (entries 4−6), the phenyl analog **2c** (entries 7−10) gave 1-phenylcyclopentene (**3c**) and *not* 3-phenylcyclopentene (**3c′**) as the major product.[6] The reversal in the regioselectivity of the 1,2 migration for the phenyl-substituted housane **2c** was certainly not expected. Since the rearrangement of a 1,3-radical cation is likely to be of the Wagner−Meerwein type (a cationic process),[2c,3] the regioselective formation of cyclopentene **3c** requires that the positive charge is essentially localized at the secondary carbon site of the 1,3-diyl radical cation and *not* at the tertiary benzylic position in the intermediate radical cation **2c**$^{\bullet+}$! Even more astonishing is the fact that the tricyclic housane **2i** (Scheme 3) gives the olefin **3i** as the sole rearrangement product (entries 26−28), in which the methyl group has migrated exclusively to the methyl-substituted site of the 1,3-diyl radical cation **2i**$^{\bullet+}$.

How can these apparently contradictory results be mechanistically rationalized? Let us consider the two possible extreme structures for the 1,3-radical cation, namely the unpaired electron located at the more or the less substituted carbon. The oxidation potentials for the *tert*-butyl, cumyl, and isopropyl radicals are 0.09,[31a] 0.16,[31a,b] and 0.47 V[31c] (against SCE). On the basis of these data one would expect that the radical cations **2b**$^{\bullet+}$, **2c**$^{\bullet+}$, and **2i**$^{\bullet+}$ should be formed on ionization of the respective triplet diradical (Scheme 4). Consequently, the 1,2 rearrangement

Scheme 3

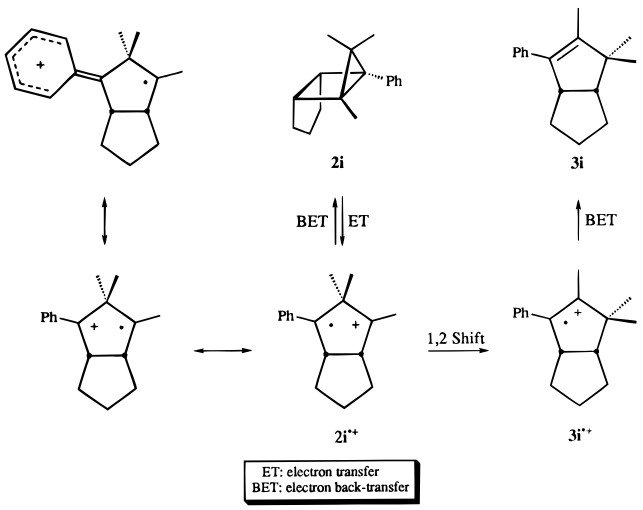

Scheme 4

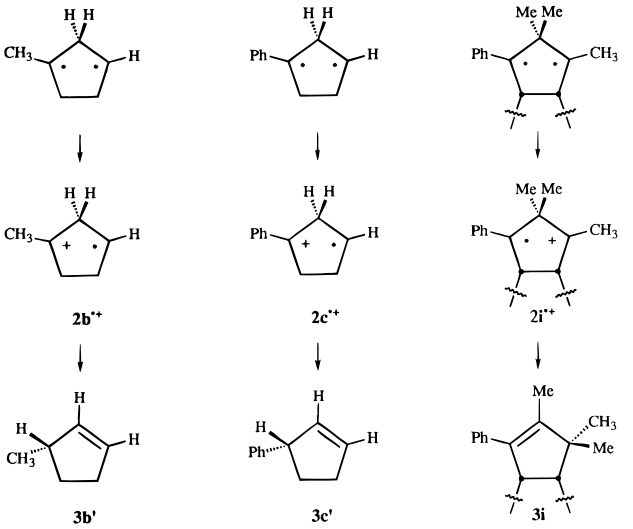

followed by BET should afford the corresponding cyclopentenes **3b′**, **3c′**, and **3i**. While this fits for the 1,3-radical cations **2b**$^{\bullet+}$ and **2i**$^{\bullet+}$, for **2c**$^{\bullet+}$, the olefin **3c** instead of **3c′** is the major regioisomeric product (entries 7−10). Similarly, an attempt to rationalize the regioselectivities in terms of reaction enthalpies for the two regioisomeric rearrangement modes also failed.[32]

AM1 calculations[33] on the radical cations **2b**,**c**,**i**$^{\bullet+}$ provide a rationale for these apparently divergent results, as reflected by the **charge** and *spin density* distributions in the radical cations (Figure 1). For the methyl derivative **2b**$^{\bullet+}$, the summed ($\sum q_i$) as well as the local (q_i) positive charges are localized on the tertiary site of the 1,3-diyl radical cation, whereas the summed ($\sum \rho_i$) and local (ρ_i) spin densities are centered mostly on the secondary center. In contrast, while the positive charge and

(31) (a) Wayner, D. D. M.; McPhee, D. J.; Griller, D. *J. Am. Chem. Soc.* **1988**, *110*, 132−137. (b) Sim, B. A.; Milne, P. H.; Griller, D.; Wayner, D. D. M. *J. Am. Chem. Soc.* **1990**, *112*, 6635−6638. (c) The experimental value seems not to be reported and a reviewer suggested the reasonable value of 0.47 V.

(32) The ΔH_f values (AM1 calculations, geometry preoptimized by AUHF, followed by RHF with one singly occupied level) for the olefin radical cations **3**$^{\bullet+}$ are 192 kcal/mol (**3b**$^{\bullet+}$), 204 kcal/mol (**3b′**$^{\bullet+}$), 214 kcal/mol (**3c**$^{\bullet+}$), 239 kcal/mol (**3c′**$^{\bullet+}$), 191 kcal/mol (**3i**$^{\bullet+}$), and 201 kcal/mol (**3i′**$^{\bullet+}$).

(33) The AM1 method was used, cf.: Dewar, M. J. S.; Zoebisch, E. G.; Healy, E. F.;Stewart, J. J. P. *J. Am. Chem. Soc.* **1985**, *107*, 3902−3909 (by employing the VAMP program on a Silicon Graphics Iris Indigo workstation: Rauhut, G.; Alex, A.; Chandrasekhar, J.; Steinke, T.; Clark, T. *VAMP 5.0*; Universität Erlangen: Erlangen, FRG, 1993).

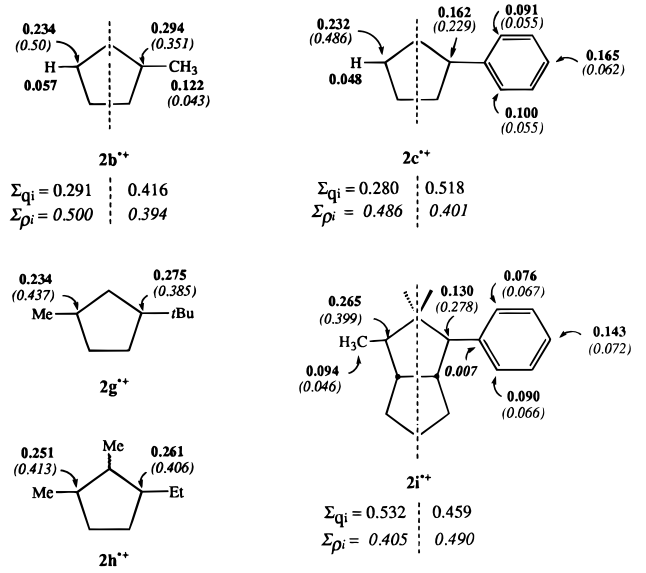

Figure 1.

the spin density on the hydrogen-bearing carbon atom for the phenyl analogue **2c**$^{\bullet+}$ are quite similar to those of the methyl derivative **2b**, on the benzylic position the differences are drastic. Although the summed positive charge is higher on the phenyl- than on the hydrogen-bearing half of the radical cation, due to delocalization into the aromatic ring, effectively the value of the local charge at the phenyl-substituted site is lower than at the hydrogen-bearing one. Accordingly, the local charge in the radical cation **2b**$^{\bullet+}$ is larger at the methyl-carrying center (0.294 *versus* 0.234), while in **2c**$^{\bullet+}$, it is larger (0.232 *versus* 0.162) at the hydrogen-substituted site. As a consequence, the larger positive charge on the secondary center in the phenyl-substituted radical cation **2c**$^{\bullet+}$ promotes preferential 1,2 hydrogen migration to afford the more substituted cyclopentene **3c**, while the larger positive charge at the tertiary site in the methyl-substituted radical cation **2b**$^{\bullet+}$ leads preferentially to the less substituted cyclopentene **3b′**.

The AM1 calculations for the bicyclic radical cation **2i**$^{\bullet+}$ predict that the summed and local positive charges are both localized on the methyl-bearing site and *not* on the benzylic position of this radical cation. Due to more effective delocalization into the aromatic ring, the difference in the local charge values for **2i**$^{\bullet+}$ (0.265 *versus* 0.130) becomes even more pronounced compared to the radical cation **2c**$^{\bullet+}$(0.232 *versus* 0.162) and, therefore, 1,2-methyl migration occurs exclusively to the methyl-bearing carbon atom. In line with this statement is also the calculated total spin density, which accumulates mostly on the phenyl-bearing half of the radical cation **2i**$^{\bullet+}$. Thus, not the charge-stabilizing ability of a substituent but the larger residual positive charge on the decisive 1,3-diyl center is responsible for the regioselectivity in the 1,2 migration.

The slight regioisomeric excess (ca. 60:40) of the rearrangement olefins **3f**−**h** over **3f**−**h′** in the case of the unsymmetrically 1,4-dialkylated bicyclopentanes **2f**−**h** (entries 17−25, Table 1) can be also rationalized in terms of better stabilization by the larger alkyl group. AM1 calculations were conducted on the radical cations **2g,h**$^{\bullet+}$ and as illustrated in Figure 1, the positive charges are for both radical cations larger at the *tert*-butyl- and ethyl-substituted carbon atoms. However, the differentiation is small and, thus, the regioselectivity in the 1,2 migration for the radical cations **3f**−**h**$^{\bullet+}$ is low (ca. 60:40), as found experimentally.

Diastereoselectivity of the 1,2 Migration in the 1,3-Diyl Radical Cations. Whereas the diastereomeric 5-methylbicyclo-

Scheme 5

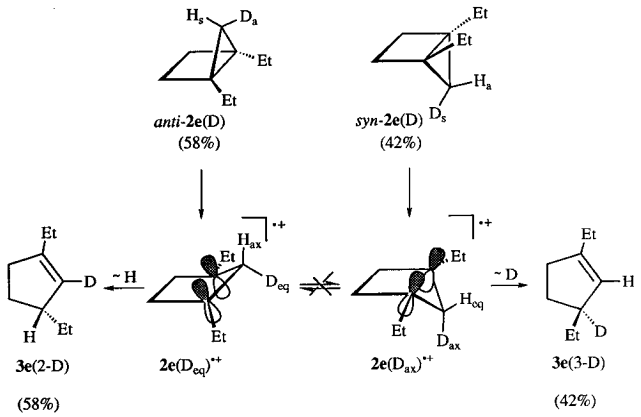

Scheme 6

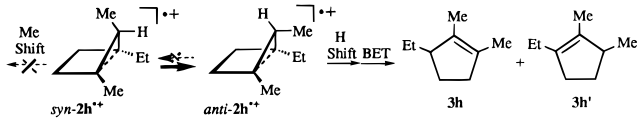

[2.1.0]pentanes readily rearranged upon γ radiolysis diastereoselectively to the corresponding cyclopentenes **3b**,**b′**,[3d] the 1,4-dimethyl derivative **2d** resisted rearrangement[3a] under matrix isolation conditions even up to 150 K, the softening point of the matrix. From the EPR results, an activation energy of at least 10 kcal/mol for rearrangement was estimated. This behavior of the radical cation **2d**$^{\bullet+}$ opens the question of, whether the previously observed diastereoselectivity of the 1,2 migration applies also in such significantly more persistent 1,3-diyl radical cations.

As presented in the Results, the CET reaction of the deuterium-labeled housane **2e**(D) conserved the initial *syn*/*anti* deuterium distribution (entries 15 and 16) of the housane **2e**(D) quantitatively in the rearrangement to the cyclopentene **3e**(D) product, as shown in eq 4. Notice that the deuterium isotope effect must be minor since the initial diastereomeric ratio in the housane **2e**(D) is identical to the final one in the resulting cyclopentene **3e**. This result establishes that the already mentioned *stereochemical memory effect*[3e] also operates in the more persistent disubstituted 1,3-diyl radical cations. Evidently,[3a] in the puckered conformation of the radical cation **2e**(D)$^{\bullet+}$, the original *syn* substituent aquires a *pseudo-axial* orientation (Scheme 5) in almost perfect coplanar alignment with the 2p orbital at the bridgehead positions, while the *pseudo-equatorial* substituent is located essentially parallel to the nodal plane of the 2p orbitals. Migration of the *pseudo-axial* substituent is favored, and this stereoelectronic control accounts for the stereoselective formation of the cyclopentenes **3e**(2-D) and **3e**(3-D) from the C-5 deuterium-labeled housanes **2e**(D).

Whereas for the methyl-stereolabeled housane *anti*-**2h** the same diastereoselectivity as above applies, for its *syn*-**2h** diastereomer, a complete reversal is observed (Scheme 6). Thus, by starting either from the *anti* isomer (entry 24), from the *syn* isomer (entry 25), or from mixtures of both (entry 21−23), exclusively the two cyclopentenes **3h**,**h′** were obtained, i.e. only a 1,2 hydrogen shift had occurred. These results indicate that the *syn* isomer of the radical cation **2h**$^{\bullet+}$ suffers irreversible ring flip to the *anti* isomer prior to rearrangement, in which the hydrogen atom is *pseudo-axial* and methyl *pseudo-equatorial* situated. Indeed, AM1 calculations show that the *anti*-**2h**$^{\bullet+}$ radical cation is by ca. 1 kcal/mol of lower energy than its *syn*-**2h**$^{\bullet+}$ diastereomer. Thus, the thermodynamically favored *pseudo-equatorial* methyl substituent will resist to acquire the

essential *pseudo-axial* orbital alignment for kinetically facile migration. Consequently, the *pseudo-axial* hydrogen atom migrates to give exclusively the cyclopentenes **3h**,**h′**, irrespective with which housane diastereomer one commences. Moreover, AM1 calculations on the resulting cyclopentene 1,2-radical cations predict that the tetraalkyl-substituted olefin radical cation (H migration) possesses ca. 12 kcal/mol less energy than the corresponding trialkyl-substituted one (Me migration).[34] This constitutes an additional substantial thermodynamic driving force in favor of hydrogen migration.

Comparison of Photoinduced Electron Transfer in Solution *versus* in the Zeolite Cavities. The TPT-photoinduced electron transfer of the bicyclopentanes **2** in the homogeneous phase yields the rearrangement olefins **3** (Table 1). In the heterogeneous phase, the most noticeable characteristic finding is that all the photolyses proceed more slowly and in slightly lower yields, presumably due to light scattering and mobility restrictions imposed by the zeolite. Nonetheless, the product distributions were not significantly different from those obtained in the homogeneous phase. Presumably, for such small molecules as the bicyclopentanes **2**, the steric effects are too small in the confined environment of the zeolite cavity to cause changes, e.g. in the diastereomeric selectivity, in the PET chemistry of the bicyclopentane derivatives.

Reduced BET for some PET reactions in zeolites has been documented.[8a,10d] It has been proposed that absorption effects of ionic species at the aluminosilicate sites and/or electrostatic fields within the zeolite supercage may be the contributing factors in the retardation of the electron transfer rate.[10d] These effects may operate within the supercage also for the present radical ion pairs, but the PET chemistry between the housanes **2** and TP^+-entrapped zeolite (Y[TP]) does not reveal it in the product data.

In summary, for the first time an extensive comparative study was conducted on the chemical and photochemical electron transfer modes for the bicyclopentanes **2** as electron donors in solution and within zeolite cavities. The CET mode constitutes the best of these for the oxidation of the bicyclopentanes **2**. In conjunction with previous[3a,e] EPR studies, the present results provide valuable mechanistic insight on the regioselectivity (effective charge localization) and diastereoselectivity (conformational *memory effect*) in the rearrangement of the intermediary 1,3-diyl radical cations to the corresponding cyclopentenes.

Acknowledgment. The Würzburg group thanks the Volkswagen-Stiftung and the Fonds der Chemischen Industrie for financial support. C.S. is grateful to the University of Würzburg for financial support (1991−1994) and M.-J.S.-P. to the Alexander von Humboldt-Stiftung for a postdoctoral fellowship (1993−1994).

Supporting Information Available: Text describing experimental data and figure showing NOE effects (14 pages). This material is contained in many libraries on microfiche, immediately follows this article in the microfilm version of the journal, can be ordered from the ACS, and can be downloaded from the Internet; see any current masthead page for ordering information and Internet access instructions.

JA950397K

(34) The ΔH_f values (AM1 calculations, see footnote 32) are 172 kcal/mol for the tetraalkyl- and 184 kcal/mol for the trialkyl-substituted olefin 1,2-radical cations.